Gaussian form of effective core potential and response function basis set derived from Troullier-Martins pseudopotential: results for Ag and Au

A. Alkauskas*, A. Baratoff, and C. Bruder

19th March 2004

Department of Physics and Astronomy, University of Basel, Klingelbergstrasse 82, CH-4056 Basel, Switzerland

Abstract

We show that the Troullier-Martins scheme for constructing scalar-relativistic density functional theory (DFT) based pseudopotentials for plane-wave calculations can be applied with equal success in gaussian-function based LCAO codes. As an example we consider the noble metals silver and gold and derive 11-electron relativistic effective core potentials, as well as a response function basis set generated by the method of Lippert *et al.* (J. Phys. Chem. **1996**, 100, 6231). With several tests we demonstrate a good performance of these effective core potentials and basis set as compared to non-DFT-based ECPs of equal quality.

1 Introduction

The low-energy physics and chemistry of molecules and solids is governed by valence electrons. The corresponding orbitals are affected by core electrons in order to ensure orthogonality to core orbitals. Pseudopo-

*Corresponding author. E-mail: audrius.alkauskas@unibas.ch

tentials or effective core potentials can represent the effect of the core electrons and decrease the computational effort by focusing on valence electrons only. Moreover, once derived from relativistic calculations, effective core potentials can include relativistic effects, which are important in heavy elements, even though non-relativistic theory is applied to valence electrons. Such potentials are referred to as RECPs.

There is an long-standing practice in the condensed matter community that pseudopotentials in plane wave calculations must be used with the density functional which was employed to generate them from a reference atomic state (for reviews on plane-wave based methods see [1, 2], and on norm-conserving pseudopotentials in plane-wave calculations [3]). This is a natural and logical choice whenever one of the plane-wave DFT codes developed by different groups is used, e.g. CPMD [4], ABINIT [5], CASTEP [6], FHI96md [7] (norm-conserving pseudopotentials), DaCapo [8], PWscf [9], VASP [10] (ultrasoft pseudopotentials). The LCAO based code SIESTA [11] employs the same numeric pseudopotentials as plane-wave based codes. An alternative approach is used in the Slater-orbital based ADF code [12], where so-called core functions are introduced. They represent the core electron charge distribution, but are not variational degrees of freedom and serve as fixed core charges which generate the potential experienced by valence electrons.

In quantum chemistry gaussian-function-based LCAO computations, effective core potentials were originally derived either from a reference calculation of a single atom within the Hartree-Fock or Dirac-Fock approximations, or from some method including electron correlations (CI, for instance). A review of these methods, as well as a general theory of ECPs is provided in [13]. Effective core potentials are based on the frozen-core approximation and serve to represent the potential generated by core electrons, also incorporating relativistic effects. So-called shape-consistent ECPs are rather easy to derive and contain no adjustable parameters. On the contrary, energy-consistent ECPs are used for high-quality studies of specific systems and specific quantities. The parameters of such ECPs and the underlying basis set can be adjusted in accordance to representative experimental data, not only for the ground state, but also for excited states, electron affinities, ionization potentials and so on. Being of semi-empirical origin, they can perform remarkably well for a given system, but their transferability to other environments can be poorer than that of shape-consistent ECPs.

The construction of shape-consistent ECPs is based on the original proposal of Christiansen-Lee-Pitzer [14] where norm-conservation was introduced. Simultaneously, norm-conserving pseudopotentials were introduced in computational condensed matter physics by Hamann *et al.* [15]. For transition metals, an analytical

form of Hartree-Fock ECPs was obtained by the Los Alamos group [16, 17].

In the past, a flurry of work dealing with noble and transition metals within DFT employed effective core potentials derived for mainstream quantum chemistry approaches. Both transport and ground state electronic structure calculations followed this way. As some examples, we mention recent studies of medium-size silver clusters [18], adsorption on gold and platinum clusters [19, 20, 21] and on platinum and silver slabs [22, 23, 24], transport through a molecular wire contacted to noble metals [25, 26, 27, 28], metalo-organic complexes [29], metal hydrides [30] and so on. The common trend to make these potentials more flexible for density-functional theory treatment is to vary exponents and contraction coefficients of gaussian primitives to attain an optimum description. However, when used with DFT, this simple adjustment of basis functions cannot cure the problem that most popular ECPs in quantum chemistry were not derived for DFT. We must mention at the outset that this issue is not so important whenever a small core can be assumed. The smaller the core, the more unimportant is the method by which ECP is derived. In the limit of a bare nucleus, the potential becomes $\sim 1/r$, which is of course independent of the method. Our primary interest is in big systems containing heavy noble and nearly-noble metals used as substrates in adsorption studies. For these metals the ns and np atomic levels lie distinctly below the nd levels ($n = 4$ for Ag and 5 for Au), whereas the $(n+1)s$ and $(n+1)p$ levels are relatively close to nd level so that states derived from all three levels overlap and significantly contribute to bonding in the bulk and at surfaces. Treating ns and np states together with lower-lying ones as belonging to the core is therefore a reasonable choice which leads to 11 electron ECPs. Including nd states in the core would require a large core radius and would ignore $sp - d$ hybridization effects which are known to be important near the Fermi level of noble metals. On the other hand, treating ns and np states as valence pseudo-orbitals, leading to 19 electron ECPs, while ensuring a small core radius, would increase computing time and storage at a cost which is not justified for most properties, except those significantly affected by the polarization of the states in question. For our purposes, 11 electron ECPs represent the best compromise.

There have been already reports by the Bonacic-Koutecky group [31, 32] about BLYP single-electron ECPs for silver and gold which were successfully applied to silver and mixed silver-gold clusters. These ECPs are energy-consistent, accordingly difficult to construct. They are intended for high-quality studies of specific properties.

Let us briefly mention existing ECPs for silver and gold:

1. Los-Alamos ECPs 11-electron ECPs [16], and 19-electron ECPs [17], designated as Lanl1DZ and Lanl2DZ. These ECPs are shape-consistent and are derived from reference calculations on an isolated atom within relativistic Dirac-Fock theory which includes mass-velocity and Darwin terms.

2. Bonacic-Koutecky 1-electron ECP for silver to be used with the BLYP functional [31, 32]. The parameters are fitted to reproduce experimental observables of small systems.

3. Bonacic-Koutecky 11-electron ECP [33] for silver, intended for usage at a correlated level of theory (MRD-CI, CCSD) and supplied with a large basis set (6s5p5d/5s3p2d). The initial parameters were taken from the Los-Alamos group and then re-optimized in accordance to experimental data.

4. Stuttgart-Dresden ECPs [34, 35], designated as SDD. These energy-consistent ECPs are constructed to reproduce experimental observables of a single atom, like ionization potentials and excitation energies, within relativistic Dirac-Fock theory.

5. Basch ECP for silver[36]; like Lanl1DZ, it is derived from relativistic Dirac-Fock calculations and replaces [Kr] core.

6. Steven-Basch-Krauss 19-electron RECPs [37], named CEP, like Lanl2DZ, they are shape consistent, derived from Dirac-Fock theory.

To the best of our knowledge, there are currently no 11-electron ECP for silver and gold derived for DFT-based methods to be used in gaussian codes. Motivated by our current interests, namely the study of adsorbed molecules on silver and gold surfaces or clusters within density-functional theory, we found the present situation unsatisfactory for our purposes. Our goal is not to construct ECPs that would rival existing ECPs for these metals, but rather to construct effective core potentials consistent with pseudopotentials extensively used with plane-waves together with a suitable Gaussian basis set that would yield a LCAO description at the same level of DFT.

All calculations have been performed with the Gaussian03 package [38].

2 Procedure

Our starting point is to chose a well-defined and well-tested pseudopotential scheme. Among several possibilities, we choose the popular and relatively simple Troullier-Martins scheme [39]. For the details of

constructing numerical Troullier-Martins pseudopotentials for the different l-channels we refer to the original article. Briefly, a pseudoorbital of angular momentum l is written in the core region as $r^l \exp[p_6(r)]$ with $p_6(r)$ being a sixth-order polynomial with seven fitting constants. The latter are adjusted to ensure norm-conservation, continuity of the pseudo-orbital, its first and second derivatives at a chosen core radius r_c, as well as other specific requirements. Then, screened pseudopotentials are derived by inverting the Schrödinger equation (using the all-electron energy eigenvalue) and transferable ionic pseudopotentials are finally obtained by subtracting from those l-dependent pseudopotentials Hartree and exchange-correlation potentials produced by pseudo-valence electrons. Atomic pseudoorbitals are therefore solutions to the single-particle radial Schrödinger equation for a screened pseudopotential, as well as solutions of the self-consistent Kohn-Sham equations for the corresponding ionic pseudopotentials. The required all-electron calculations are performed in the spin-restricted formalism (with half occupancies allowed) and scalar-relativistic mass-velocity and Darwin terms are included in the radial Kohn-Sham equation:

$$\left[\frac{1}{2M(r)}\left(-\frac{d^2}{dr^2}-\frac{1}{2M(r)c^2}\frac{dV_{eff}(r)}{dr}r\frac{d}{dr}\frac{1}{r}+\frac{l(l+1)}{r^2}\right)+V_{eff}(r)-\varepsilon_i\right]u_{nl}(r)=0, \tag{1}$$

where $V_{eff}(r)$ is the effective Kohn-Sham potential, and $M(r) = 1 + (\varepsilon_i - V_{eff}(r))/2c^2$.

2.1 Effective core potentials

To perform all-electron calculations and construct a numerical Troullier-Martins DFT pseudopotential we use the well-tested and widely used fhi98PP code [40]. In this article we present results obtained with the BLYP generalized-gradient functional [41, 42].

We choose the f ($l = 3$) component to be local and equal to the bare core potential:

$$V_L(r) = -\frac{Z}{r}. \tag{2}$$

In our case $Z = 11$; the l-dependent components for lower angular momentum channels are defined as:

$$V_{l-L}(r) = V_l^{TM}(r) + \frac{Z}{r}, \tag{3}$$

where $l = 0, 1, 2$ (s,p,d) and TM stands for Troullier-Martins. Since the latter pseudopotentials are finite at

the origin, $V_{l-L}(r)$ behave like r^{-1} as $r \to 0$ in contrast to Stuttgart-Dresden or Los Alamos ECPs, which diverge like r^{-2}. In a similar manner to those ECPs we expand these projections as a finite sum of weighted Gaussians multiplied by the Jacobian weighting factor r^2:

$$U_{l-L}(r) = V_{l-L}(r)r^2 = \sum_k b_k r^{n_k} e^{-\zeta_k r^2}, \tag{4}$$

where $n_k = 1$ for $k = 1$ and $n_k = 2$ otherwise. The expansion coefficients b_k's and exponents ζ_k's are to be determined by a suitable fitting procedure. Of course, the parameters are different for different l-components.

2.2 Basis set

Troullier-Martins, as well as all norm-conserving pseudopotentials, share the property that logarithmic derivatives of pseudo and all-electron orbitals for a given l are equal at the appropriate core radius and reference energy (atomic eigenvalue). This property strictly applies in the limit of a full basis set. In practice one can make use of norm-conservation if a rather good basis set is chosen.

There are many ways to generate a suitable and compact basis set for a given problem (see, e.g., [43, 44] and references therein). To derive a basis set consistent with a given ECP and a given density functional, we follow the systematic procedure of Lippert *et al.* [46]. Their construction is based on response functions of a given atom which describe the linear, quadratic, cubic, etc. response to an external perturbation. Linear response functions are closely connected to the so-called chemical hardness [47], a useful concept for molecular systems when interactions between subsystems is weak. Assuming that an atom is subject to an external perturbation parametrized by t, Kohn-Sham orbitals can be expanded in a Taylor series with respect to the perturbation:

$$\psi(t) = \psi(0) + t\frac{\partial\psi}{\partial t} + \frac{t^2}{2}\frac{\partial^2\psi}{\partial t^2} + ... \tag{5}$$

Lippert *et al.* showed that the local atomic basis set

$$\psi, \quad \tfrac{\partial\psi}{\partial t}, \quad \tfrac{\partial^2\psi}{\partial t^2}, \quad ... \tag{6}$$

provides a rapidly convergent description of the atom embedded in a molecule or a solid. Here we apply this

procedure for a pseudoatom keeping only linear terms. A similar procedure was applied for pseudo-atom calculations to generate basis functions for $O(N)$ calculations in [48]. As the perturbation, we consider the change in partial occupancies of atomic s and p states, the total charge being conserved.

To be specific, s and d basis functions are derived by a least-squares fit of a finite sum of primitive gaussians to numerical Troullier-Martins pseudoorbitals, that is:

$$\psi_l(r) = \sum_i c_{il} g_l(\alpha_{il}, r), \tag{7}$$

where $l = 0$, 2 and g_l stand for normalized primitive gaussians with exponents α_{il}. Linear response s and d functions which we call s^+ and d^+ are derived by performing a spin-restricted calculations of an atom with occupancy of d set to 10.0, but occupancies of s and p set to 0.95 and 0.05 respectively. From the resulting numerical pseudoorbitals ψ', linear response functions are obtained by a least-squares fit of the difference:

$$\psi_l^+(r) = N(\psi_l(r) - \psi_l'(r)) = \sum_i d_{il} g_l(\beta_{il}, r), \tag{8}$$

N being a normalization factor. Polarization functions p and p^+ are derived making use of the known result that the partial occupancy of the valence p atomic state in solid silver and gold is approximately 0.3 [49]. Therefore, we performed atomic calculations with occupancies of s and p states set to 0.7,0.3 as well as 0.65, 0.35, respectively and derived pseudoorbital and linear response functions p and p^+ by a similar fitting procedure. Choosing 3 primitive gaussians we obtain compact basis sets ($6s6p6d/2s2p2d$) for silver and ($6s6p5d/2s2p2d$) for gold. If necessary, more basis functions can be added by slightly modifying the procedure.

3 Results

3.1 ECPs

Numerical Troullier-Martins pseudopotentials for silver are plotted in Fig. 1. There is still freedom in constructing a pseudopotential given a well-defined scheme, namely, choosing the core radii at which all-electron and pseudoatom Kohn-Sham orbitals are matched. Usually, the bigger the radius, the smoother the pseudopotentials, and hence the lower the cutoff for plane-wave calculations. On the contrary, the

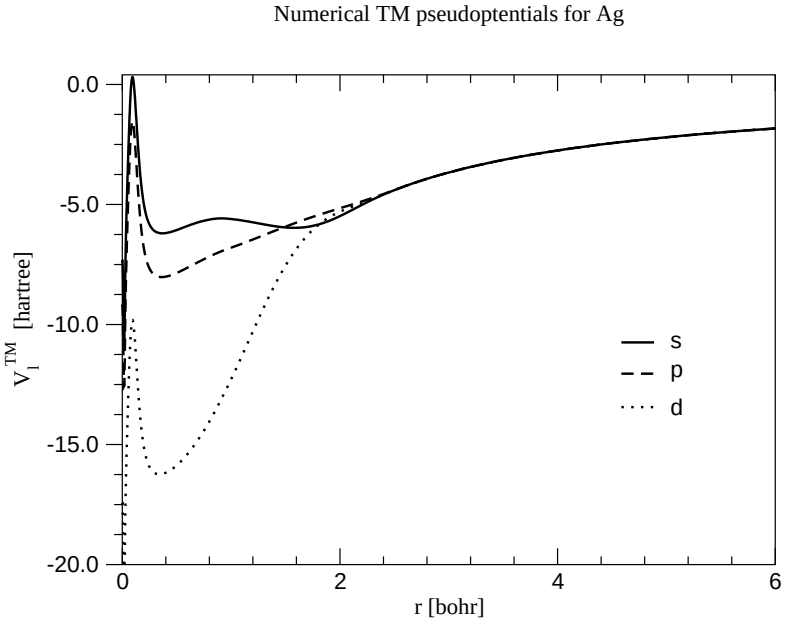

Figure 1: Numerical Troullier-Martins pseudopotentials for silver.

smaller the core radius, the harder the pseudopotentials, but the better their transferability. In plane-wave codes, constructing a pseudopotential is therefore a trade-off between those two extremes. In the LCAO formulation wavefunctions need not to be smooth, and therefore transferability can be better. Nevertheless, for a meaningful comparison we choose core radii to be the same as used in plane-wave calculations, namely 2.40 bohr for s and d, and 2.60 bohr for p states.

The different l-components as well as gaussian fits in the case of silver are depicted in Fig. 2. In the course of our work, we found that fitting a numerical ECP to a sum of gaussians is by far the most delicate task. It appeared easier to fit the wavefunctions than ECPs. Non-linear fits were performed with the help of the Grace package [50], using the Levenberg-Marquardt algorithm without weighting function. It is also more important to get accurate fits for the pseudopotentials, since SCF calculations are variational in orbital space, but not in pseudopotentials. As a result, the performance of a given ECP will largely depend on the

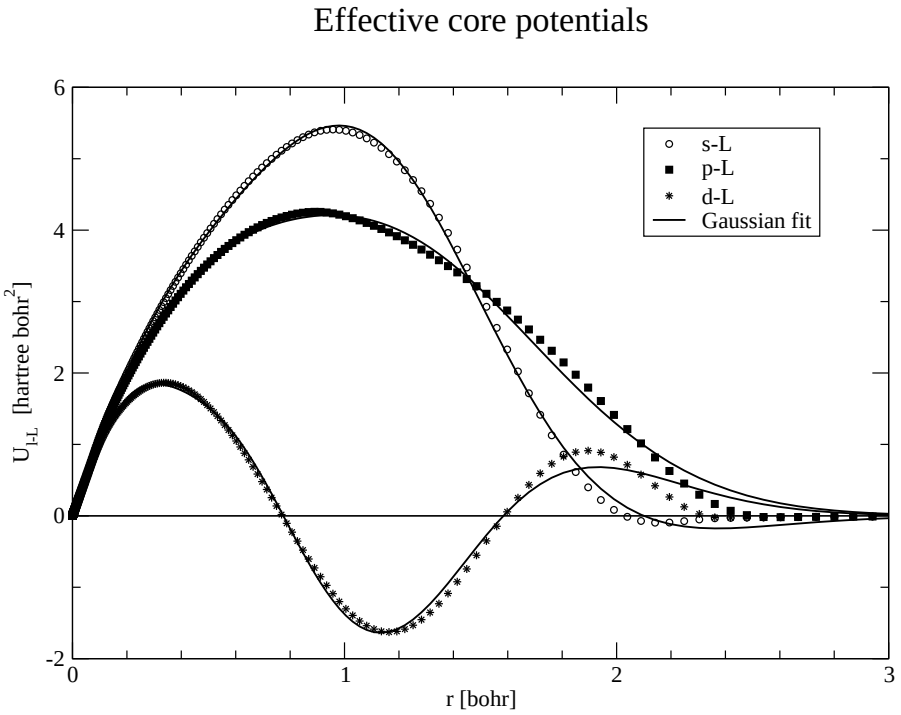

Figure 2: Effective core potentials times r^2 for silver. Symbols show numerical values, and solid lines represent analytical fits.

care devoted to the fitting procedure, for which sophisticated algorithms might improve the quality of the fit.

The parameters of our ECPs for silver are presented in Table 1 and those for gold in Table 2. The coefficients b_1 of Eq. (4) are close to 11.0 because $n_1 = 1$, whereas $n_k = 2$ for $k > 1$. Instead of insisting $b_1 = Z$ to we treat all b_k's as ζ_k's as adjustable parameters in order to obtain the best possible agreement in the range where each of the U_{l-L} is large.

	$s-L$			$p-L$			$d-L$		
k	n_k	ζ_k	b_k	n_k	ζ_k	b_k	n_k	ζ_k	b_k
1	1	1.712	11.074	1	0.897	11.074	1	12.668	9.524
2	2	1.391	−166.201	2	1.2260	−22.6472	2	1.662	227.659
3	2	1.194	255.676	2	0.9789	16.8557	2	1.400	−363.576
4	2	1.033	−91.757	-	-	-	2	1.205	150.286

Table 1: ECP parameters for silver.

	$s-L$			$p-L$			$d-L$		
k	n_k	ζ_k	b_k	n_k	ζ_k	b_k	n_k	ζ_k	b_k
1	1	2.286	10.881	1	1.380	10.721	1	11.000	9.383
2	2	1.088	−97.386	2	1.111	−63.222	2	1.660	225.822
3	2	1.267	270.134	2	0.987	60.634	2	1.342	286.233
4	2	1.499	−171.733	-	-	-	2	1.437	−497.561

Table 2: ECP parameters for gold.

3.2 Basis set

The pseudoorbitals and linear response orbitals of silver are plotted in Fig. 3. The p function is the most diffuse, showing the fact that it is weakly bound, while the d function is highly localized. The node of the s^+ function occurs at approximately 3.2 bohr, that of the p^+ function at 5.1 bohr, and of the d^+ function at 2.0 bohr, which is almost the extent of the pseudoorbitals themselves. Parameters of the response function basis set of double-zeta quality are presented in Tables 3 and 4.

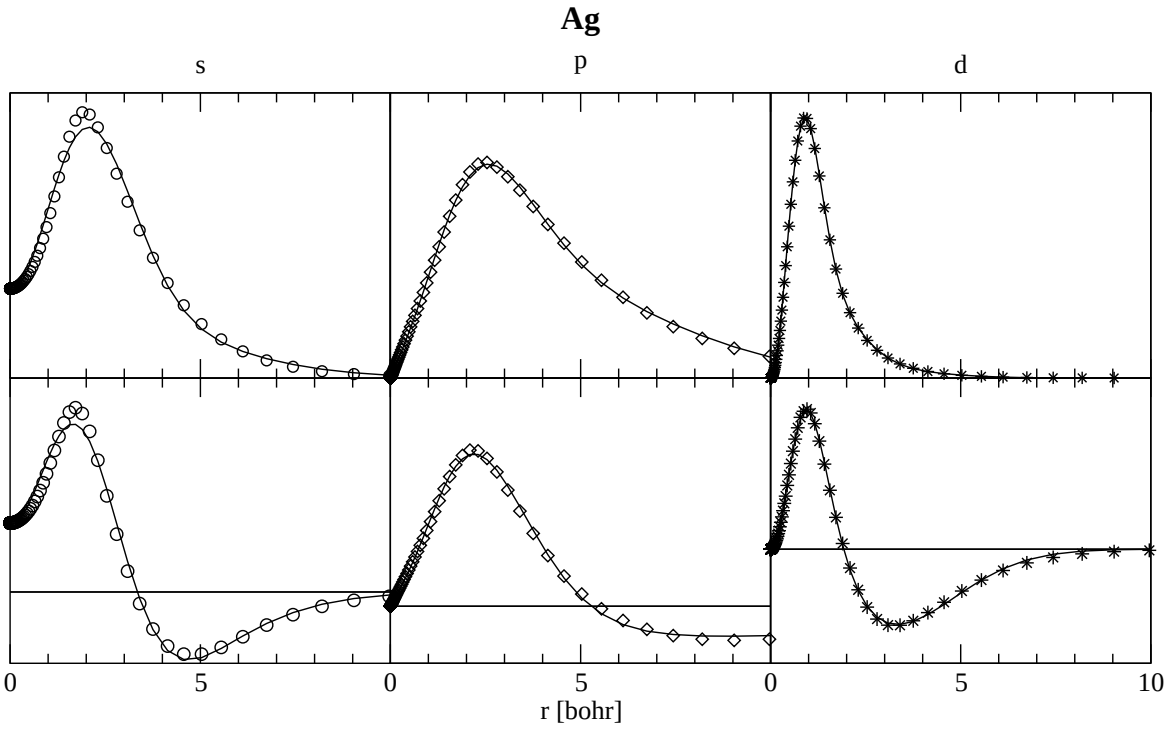

Figure 3: Ag pseudoorbitals (top) and linear response orbitals (bottom) . Symbols show numerical values, and solid lines represent analytical fits.

	s		p		d	
i	α_{i0}	c_{i0}	α_{i1}	c_{i1}	α_{i2}	c_{i2}
1	0.2453	−2.8644	0.4583	−0.0478	1.3546	0.6361
2	0.2023	3.29386	0.1198	0.4529	0.4226	0.4217
3	0.0365	0.49972	0.0274	0.6994	0.1271	0.1444
	s^+		p^+		d^+	
i	β_{i0}	d_{i0}	β_{i1}	d_{i1}	β_{i2}	d_{i2}
1	0.2725	−2.4880	0.5756	−0.0417	1.1744	0.2168
2	0.1765	4.4625	0.1224	0.59572	0.6084	0.1877
3	0.0570	−2.0099	0.0067	−0.8984	0.0982	−1.0009

Table 3: Parameters of the response function basis set for silver .

	s		p		d	
i	α_{i0}	c_{i0}	α_{i1}	c_{i1}	α_{i2}	c_{i2}
1	0.2668	−2.9011	0.3837	−0.0770	1.2109	0.5513
2	0.2137	3.4494	0.1268	0.4872	0.4059	0.4709
3	0.0354	0.3681	0.0290	0.6863	0.1257	0.1801
	s^+		p^+		d^+	
i	β_{i0}	d_{i0}	β_{i1}	d_{i1}	β_{i2}	d_{i2}
1	0.2870	−2.9512	0.4947	−0.0700	0.8854	0.4146
2	0.1870	5.5399	0.1306	0.6590	0.08670	−0.9702
3	0.0750	−2.6642	0.0084	−0.8922	-	-

Table 4: Parameters of the response function basis set for gold .

4 Test results

In this section we discuss test results for several simple silver and gold systems. Results obtained with different ECPs are comapred. In the following table the present ECPs are denoted as TM (Troullier-Martins), and SZ (single-zeta) or DZ (double-zeta). For atoms, a very big basis set including twelve gaussians (for each of s, p, and d functions) was also tested in the case of TM and Lanl1 ECPs.

4.1 Atomic tests

Results for the silver atom are presented in Table 5. We did not consider numerical ionization potentials (IPs) and electron affinities (EAs) mainly because neutral atom calculations were performed in the spin-restricted formalism (spin-singlet state with half occupancies). This raises the energy of an isolated atom and therefore decreases the IP value and increases the EA value. Numerical Kohn-Sham eigenenergies are close to those of TMSZ and TMDZ; SDD also shows very good agreement, while Lanl2DZ slightly overbinds d-states. Lanl1DZ performs very poorly, over-binding d-states and under-binding the s-state, thus giving rise to a $s-d$ difference of 5.88eV, which can lead to a poor description of $s-d$ hybridization in polyatomic systems. Even when the large 12Z basis set is used in conjunction with TM and Lanl1 ECPs, the trends remain the same. Compared to experimental IP and EA values, all ECPs with double-zeta basis sets (except Lanl1DZ) show a good agreement. Lanl1DZ, on the contrary, underestimates IP and severely underestimates EA; TMSZ, being of "minimal" nature, performs not too well either, but gives some improvement over Lanl1DZ. The same tendencies are apparent for the gold atom (Table 9). For the eigenvalues, SDD and TMDZ perform very well, while Lanl2DZ slightly overbinds d-states. Lanl1DZ again overbinds d-states and underbinds s-state. For IPs and EAs, Lanl2DZ, SDD and TMDZ perform very alike, while Lanl1DZ fails once again. Given that SDD, CEP and Lanl2DZ are 19-electron ECPs, the good performance of 11-electron ECP TMDZ is encouraging.

4.2 Diatomic molecules

Turning now to properties of dimers, for Ag_2 the performance of TMDZ is poorer than that of Lanl2DZ and SDD if compared to experimental results. Lanl1DZ performs worse that TMSZ, but keeping in mind the underbinding tendency of the BLYP functional [51], the larger-than-experimental values of binding energies

	$\varepsilon_{4d\uparrow}$[eV]	$\varepsilon_{4d\downarrow}$[eV]	$\varepsilon_{5s\uparrow}$[eV]	$E_{tot}[a.u.]$	IP [eV]	EA [eV]
Numerical value	-7.34		-4.45	-35.9900	-	-
Lanl1DZ	-9.80	-9.67	-3.92	-38.9551	6.97	0.39
Lanl2DZ	-7.46	-7.32	-4.60	-145.6558	7.80	1.10
Lanl1-12Z	-9.75	-9.62	-3.94	-39.9621	7.05	0.97
SDD	-7.30	-7.13	-4.73	-146.9080	8.08	1.43
CEP	-7.13	-6.97	-4.53	-146.1825	7.88	1.06
TMSZ	-7.42	-7.20	-4.67	-35.9650	8.14	0.63
TMDZ	-7.34	-7.16	-4.66	-35.9652	7.92	1.18
TM-12Z	-7.23	-7.05	-4.72	-35.9797	8.03	1.42
Exp.	-	-	-	-	7.58	1.30

Table 5: Comparison of Kohn-Sham eigenenergies, ionization potentials and electron affinities of the Ag atom

ECP	r_e $[A]$	D_e[eV]	ω_e[cm^{-1}]
Lanl1DZ	2.75	1.26	131
Lanl2DZ	2.62	1.69	174
SDD	2.60	1.66	175
CEP	2.62	1.68	172
TMSZ	2.71	1.41	157
TMDZ	2.67	1.48	164
Exp.	2.50	1.67	192

Table 6: Comparison of equilibrium distances r_e, binding energies D_e, and vibrational frequencies ω_e for the Ag_2 dimer.

obtained with Lanl2DZ and CEP seem to indicate an intrinsic deficiency of these ECPs when used with DFT. For Au_2 (Table 10), all ECPs seem to perform rather well; SDD, CEP and Lanl2DZ yield a somewhat better agreement, while Lanl1DZ fails here also. For the case of AgH (Table 7), Lanl2DZ and SDD perform slightly better than TMDZ, but the latter gives significant improvement over Lanl1DZ. The dipole moments predicted by of all the ECPs, except Lanl1DZ, are close to each other.

It is very important to test molecules, in which charge transfer is expected to be significant. Results for the molecules AgCl and AuF are presented in Tables 8 and 11, respectively. Compared to Lanl2DZ, CEP and SDD, TMDZ shows the same trends as in Ag_2 and Au_2: equilibrium distances are slightly larger, binding energies and vibrational frequencies slightly smaller, but dipole moments are similar, as well as Mulliken charges on chlorine and fluorine atoms.

We note, however, that the comparison of different ECPs with plain wave calculations should be viewed

ECP	r_e [A]	D_e[eV]	ω_e[cm^{-1}]	μ_e[D]	Δq_H
Lanl1DZ	1.77	2.08	1385	3.25	-0.06
Lanl2DZ	1.64	2.49	1702	2.55	$+0.03$
SDD	1.63	2.56	1765	2.31	$+0.05$
CEP	1.64	2.44	1742	2.40	$+0.03$
TMSZ	1.69	2.26	1643	2.45	$+0.01$
TMDZ	1.68	2.37	1640	2.40	$+0.02$
Exp.	1.62	2.39	1760	-	-

Table 7: Comparison of equilibrium distances r_e, binding energies D_e, vibrational frequencies ω_e, dipole moments μ_e, and Mulliken charges on the hydrogen atom Δq_H for the AgH molecule.

ECP	r_e [A]	D_e[eV]	ω_e[cm^{-1}]	μ_e [D]	Δq_{Cl}
Lanl1DZ	2.47	2.91	282	6.30	-0.39
Lanl2DZ	2.41	2.76	308	5.29	-0.28
SDD	2.38	2.82	312	5.05	-0.25
CEP	2.39	2.83	314	5.04	-0.30
TMSZ	2.46	2.51	288	5.06	-0.35
TMDZ	2.45	2.67	292	5.15	-0.33
Experimental	2.28	3.24	344	5.73	-

Table 8: Comparison of equilibrium distances r_e, binding energies D_e, vibrational frequencies ω_e, dipole moments μ_e, and Mulliken charges on the chlorine atom Δq_{Cl} for the AgCl molecule.

	$\varepsilon_{4d\uparrow}$[eV]	$\varepsilon_{4d\downarrow}$[eV]	$\varepsilon_{5s\uparrow}$[eV]	E_{tot}[$a.u.$]	IP [eV]	EA [eV]
Numerical value	-6.76		-5.77	-32.9259	-	-
Lanl1DZ	-8.88	-8.66	-4.80	-34.7921	8.24	0.86
Lanl2DZ	-7.14	-6.92	-6.07	-135.3516	9.49	2.22
Lanl1-12Z	-8.80	-8.58	-4.87	-34.8028	8.28	1.52
SDD	-6.93	-6.69	-5.95	-135.6906	9.53	2.29
CEP	-6.72	-5.78	-6.49	-136.0018	9.39	2.03
TMSZ	-7.00	-6.70	-5.96	-32.9691	9.82	1.54
TMDZ	-6.93	-6.65	-5.95	-32.9693	9.50	2.15
TM-12Z	-6.80	-6.53	-6.08	-32.9836	9.66	2.39
Exp	-	-	-	-	9.23	2.31

Table 9: Comparison of Kohn-Sham eigenenergies, ionization potentials, and electron affinities for the Au atom.

ECP	r_e $[A]$	D_e[eV]	$\omega_e[\mathrm{cm}^{-1}]$
Lanl1DZ	2.74	1.53	138
Lanl2DZ	2.58	1.99	156
SDD	2.60	2.00	158
CEP	2.59	2.06	159
TMSZ	2.65	1.74	148
TMDZ	2.62	1.85	153
Exp.	2.47	2.29	191

Table 10: Comparison of equilibrium distances r_e, binding energies D_e, and vibrational frequencies ω_e for the Au_2 dimer.

ECP	r_e $[A]$	D_e[eV]	$\omega_e[\mathrm{cm}^{-1}]$	$\mu_e[D]$	Δq_F
Lanl1DZ	2.17	2.83	469	4.44	-0.34
Lanl2DZ	2.00	2.80	497	3.38	-0.30
SDD	2.00	3.11	512	3.75	-0.26
CEP	2.00	2.98	534	3.47	-0.28
TMSZ	2.05	2.42	483	3.12	-0.30
TMDZ	2.03	2.87	510	3.58	-0.27
MP4 [52]	1.94	3.05	540	5.00	-

Table 11: Comparison of equilibrium distances r_e, binding energies D_e, vibrational frequencies ω_e, dipole moments μ_e, and Mulliken charges on fluorine atom Δq_F for the AuF molecule.

with some care. Lanl2DZ, SDD and CEP include semicore states and there is an energy gain because of the semicore polarization. In contrast, no semicore states are included in our plane wave calculations, TM and Lanl1 ECPs, but plane wave basis set naturally includes all polarization functions (f and higher) which are not included in any of the ECPs. Nevertheless, in our opinion, the adopted method of constructing effective core potentials and basis functions for gaussian codes has the advantage of being systematic and thus open for improvement.

5 Conclusions

We have shown how Troullier-Martins pseudopotentials, generated for a particular functional, can be used to construct effective core potentials for gaussian-based codes. Going beyond the present double-zeta level, basis sets of triple-zeta and higher quality, as well as polarization functions can be constructed by similar means. Our 11-electron ECPs are not expected to perform better than 19-electron ECPs (both semi-empirical like SDD or shape-consistent like Lanl2DZ), but give significant improvement over non-DFT derived 11-electron ECPs and are expected to give results similar to plane-wave calculations. They can be thus used for studies of larger systems, like molecules adsorbed on noble metal clusters and slabs. We tested the performance of these ECPs (together with a double-zeta response function basis set) for small systems containing silver and gold atoms and showed them to perform well as opposed to results obtained with an 11-electron ECP derived from Hartree-Fock calculation (Lanl1DZ). This clearly demonstrates that the derivation of ECPs and their application should be based on the same model chemistry.

6 Acknowledgments

We acknowledge financial support from the Swiss National Science Foundation through its NCCR for Nanoscale Science, and the Computing Center of the University of Basel for computational resources. We would like to thank S. Goedecker for discussions and for pointing out Ref. [46].

References

[1] D. Marx and J. Hutter, in *Modern Methods and Algorithms of Quantum Chemistry*, NIC Series, **2000**, Vol. 3.

[2] M. E. Tuckermann, J. Phys. Cond. Mat. **2002**, 14, R1297.

[3] M. Fuchs, M. Bockstedte, E. Pehlke, M. Scheffler, Phys. Rev. B **1998**, 57, 2134.

[4] CPMD, J. Hutter *at al*, Copyright IBM Corp **1990-2001**, Copyright MPI fur Festkorperförschung Stuttgart 1997-2001; *http://www.cpmd.org.*

[5] ABINIT, *http://www.abinit.org.*

[6] CASTEP, *http://www.tcm.phy.cam.ac.uk/castep.*

[7] FHI96md, *http://www.fhi-berlin.mpg.de/th/fhimd.*

[8] DaCapo, *http://www-ali.cs.umass.edu/DaCapo.*

[9] PWscf, *http://www.pwscf.org.*

[10] VASP, *http://www.cms.mpi.univie.ac.at/vasp.*

[11] SIESTA, *http://www.uam.es/departamentos/ciencias/fismateriac/siesta.*

[12] ADF, *http://www.scm.com.*

[13] M. Dolg, in *Modern Methods and Algorithms of Quantum Chemistry*, NIC Series **2000**, Vol. 3.

[14] A.P. Christiansen, Y.S. Lee, K.S. Pitzer, J. Chem. Phys. **1979**, 71, 4445.

[15] D.R. Hamann, M. Schluter, C. Chiang, Phys. Rev. Lett. **1979**, 43, 1494.

[16] P.J. Hay, W.R. Wadt, J. Chem. Phys. **1985**, 82, 270.

[17] P.J. Hay, W. R. Wadt, J. Chem. Phys. **1985**, 82, 299.

[18] R. Fournier, J. Chem. Phys. **2001**, 115, 2165.

[19] C.W. Bauschlicher, A. Ricca, Chem. Phys. Lett. **2003**, 367, 90.

[20] A. Ricca, C.W. Bauschlicher, Chem. Phys. Lett. **2003**, 372, 873.

[21] V. Bertani, C. Cavallotti, M. Masi, S. Carra, J. Phys. Chem. A **2000**, 104, 11390.

[22] Y. Akinaga, T. Nakajima, K. Hirao, J. Chem. Phys. **2001**, 114, 8555.

[23] K. Doll, N.M. Harrison, Phys. Rev. B **2001**, 63, 165410.

[24] K. Doll, Phys. Rev. B **2002**, 66, 155421.

[25] P.S. Damle, A.W. Ghosh, S. Datta, Phys. Rev. B **2001**, 64, 201403.

[26] J. Heurich, J. C. Cuevas, W. Wenzel, G. Schön, Phys. Rev. Lett. **2002**, 88, 256803.

[27] C. W. Bauschlicher, A. Ricca, N. Mingo, J. Lawson, Chem. Phys. Lett. **2003**, 372, 723.

[28] Y.Q. Xue, M.A. Ratner, Phys. Rev. B **2003**, 68, 115406.

[29] I. P. Georgakaki , L.M. Thomson, E.J. Lyon, M.B. Hall, M.Y. Darensbourg, Coordin. Chem. Rev. **2003**, 238, 255.

[30] L. Joubert, P. Maldivi, J. Phys. Chem. A **2001**, 105, 9068.

[31] R. Mitric, M. Hartmann, B. Stanca, V. Bonacic-Koutecky, P. Fantucci, J. Phys. Chem. A **2001**, 105, 8892.

[32] V. Bonacic-Koutecky, J. Burda, R. Mitric, M. Ge, G. Zampella, P. Fantucci, J. Chem. Phys. **2002**, 117, 3120.

[33] V. Bonacic-Koutecky, J. Pittner, M. Bairon, P. Fantucci, J. Chem. Phys. **1999**, 110, 3876.

[34] M. Dolg, U. Wedig, H. Stoll, H. Preuss, J. Chem. Phys. **1987**, 86, 866.

[35] D. Andrae, U. Haussermann, M. Dolg, H. Stoll, H. Preuss, Theor. Chim. Acta **1990**, 77, 123.

[36] H. Basch, J. Am. Chem. Soc. **1981**, 103, 4657.

[37] W.J. Stevens, M. Krauss, H. Basch, P.G. Jasien, Can. J. Chem. **1992**, 70, 612.

[38] Gaussian 03, Revision B.01, M. J. Frisch *et al.*, Gaussian, Inc., Pittsburgh PA, **2003**.

[39] N. Troullier, J. L. Martins, Phys. Rev. B **1991**, 43, 1993.

[40] M. Fuchs, M. Scheffler, Comp. Phys. Comm. **1999**, 119, 67.

[41] A.D. Becke, Phys. Rev. A **1988**, 38, 3098.

[42] C. Lee, W. Yang, R.G. Parr, Phys. Rev. B **1988**, 37, 758.

[43] W.J. Hehre, L. Radom, P.R. Scheyler, J.A. Pople, *Ab initio* molecular *orbital theory*, John Wiley & Sons **1986**.

[44] E. R. Davidson, D. Feller, Chem. Rev. **1986**, 86, 681.

[45] F. Jensen, *Introduction to computational chemistry*, John Wiley & Sons **2001.**

[46] G. Lippert, J. Hutter, P. Ballone, M. Parrinello, J. Phys. Chem. **1996**, 100, 6231.

[47] R.G. Parr, R.G. Pearson, J. Am. Chem. Soc. **1983**, 105, 7512.

[48] E. Anglada, J.M. Soler, J. Janquera, E. Artacho, Phys. Rev. B **2002**, 66, 205101;

[49] D. A. Papaconstantopoulos, *Handbook of the band structure of elemental solids*, Plenum Press, New York **1986**.

[50] Grace, *http://plasma-gate.weizmann.ac.il/Grace*.

[51] W. Koch, M.C. Holthausen, *A Chemist's Guide to Density Functional Theory*, Wiley-VCH,Weinheim **2001**.

[52] P. Schwerdtfeger, J.S. McFeaters, M.J. Liddell, J. Hrusak, H. Schwarz, J. Chem. Phys. **1995**, 103, 245.